

Research Article



Biomedical Applications of Calcium Oxide Nanoparticles - A Spectroscopic Study

Suja Abraham*, V P Sarathy

Department of Physics, Faculty of Science, Hindustan Institute of Technology and Science, India.

*Corresponding author's E-mail: sujaabrahamthuthiyil@gmail.com

Received: 08-02-2018; Revised: 30-02-2018; Accepted: 15-03-2018.

ABSTRACT

Nanoparticles (NPs) have potential applications in biomedical field. Among the nano metal oxide NPs, CaO NPs can be used as an antimicrobial agent, a potential drug delivery agent as well as in various other biomedical applications. The conformational behavior of albumin on conjugation with NPs is very important for designing and fabricating nano composites in various biomedical applications. Therefore, interaction of bovine serum albumin (BSA) with CaO NPs and effect of CaO NPs in the structure of BSA was studied by spectroscopic techniques. CaO NPs prepared by precipitation method were characterized by techniques XRD, FTIR and TEM. Conformational changes of BSA induced by CaO NPs were observed during the interaction studies.

Keywords: Protein, Calcium oxide nanoparticles, XRD, Fluorescence, Conformational changes.

INTRODUCTION

Nanotechnology has wide applications in different fields of science and technology and current research is focused on NP based products and their applications. Most of the biological molecules size is similar to that of NPs hence it can be used for both in vivo and in vitro biomedical research and applications. NPs, “a wonder of nano medicine” have potential applications in drug delivery,¹ cancer therapeutics,² to target bacteria as an alternative to antibiotics and in antibacterial vaccines to control bacterial infections.³ Inorganic nano metal oxide NPs (TiO₂, MgO, CaO, CuO and ZnO) have distinct features and are safe, stable and possess multifunctional properties. These NPs are well known for their inherent antimicrobial activity and have potential applications in food, environment and healthcare.⁴ Among these, CaO NPs possess excellent antimicrobial potential and capability to inactivate microbial endotoxin.^{5,6} Due to CaO NPs unique structural and optical properties they can be used as a potential drug delivery agent,⁷ in photodynamic therapy (PDT), photo-thermal therapy (PTT), and synapic delivery of chemotherapeutic agents.⁸ CaO NPs are safe material to human beings and animals.

In various biomedical applications conformational change of albumin on interaction with NPs plays a key role. BSA is a good model to study protein conformational changes due to its wide range of physiological functions, an ideal protein for intrinsic fluorescence measurements, well characterized structure and property and readily undergoes conformational changes.⁹ Most of the therapeutic nanosystems are designed for intravenous systemic administration, targeting the desired organ. When NPs enter a biological fluid there will be changes in conformation and biological activity of proteins as well as modification in the properties of NPs.¹⁰ Thus stabilization of the system as well as introduction of biocompatible

functionalities into these NPs for further biological interactions or coupling takes place by conjugation of protein with NPs which will help better design and fabricate nanocomposites for applications in diagnostics, drug delivery and cell monitoring. Therefore, in the present study interaction of CaO NPs with BSA was studied by spectroscopic techniques. To the best of our knowledge fluorescence measurements of BSA – CaO complex is reported for the first time.

MATERIALS AND METHODS

Chemicals

BSA was purchased from Sigma- Aldrich, USA. All other chemicals were purchased from SD fine chemicals, India.

Preparation of CaO NPs

The required amount of calcium chloride dihydrate was dissolved in deionized water under constant stirring. The stirring was continued until complete dissolution of calcium chloride precursor. Then 1 M sodium hydroxide was added slowly into the above calcium chloride containing aqueous solution at 80°C under vigorous stirring. The white precipitate of calcium hydroxide was formed while adding NaOH. Finally, addition of NaOH was stopped at pH 11.2. Now, the precipitate was allowed to settle down for some time. Afterwards, precipitate was filtered and rinsed several times with distilled water until the unreacted products were washed away. This product was dried at 100°C overnight and it was grounded well using agate mortar. The resultant fine powder of Ca(OH)₂ was calcinated in muffle furnace at 600°C for 3 h. During calcination, the calcium hydroxide was decomposed into calcium oxide. Thus prepared calcium oxide was used for further characterization.



Stock preparation and interaction of BSA with CaO NPs

Among the prepared stock solutions of BSA and CaO NPs, CaO NPs were subjected to ultrasonic vibration for 20 minutes. The mixture of BSA with various concentrations of CaO NPs were homogenized and kept for 30 min for incubation. The emission spectra were taken in the range 310-420nm at an excitation wavelength of 290 nm. Double distilled water was used for interaction studies. All measurements were performed at room temperature.

Characterization

XRD

The structure of CaO was confirmed using Brucker K 8600 X-ray diffractometer in the 2θ range of 20° to 70° .

FTIR

FTIR measurements were taken by Thermo Nicolet Avatar 370 FTIR spectrometer.

TEM

The particle size of the prepared nano- sized CaO was estimated with the help of JEOL JSM 5610 LV tunneling electron microscope.

Steady state fluorescence measurements

JASCO FP – 8600 spectrofluorometer was used for fluorescence measurements. The excitation slit width 2.5 nm, emission slit width 2 nm and scan rate 500 nm/min were maintained constant for all measurements.

Time resolved fluorescence measurements

Picosecond time correlated single photon counting (TCSPC) spectrometer was used for fluorescence lifetime measurements. The excitation source is the tunable Ti-sapphire laser (Tsunami, Spectra Physics, USA).

RESULTS AND DISCUSSION

XRD analysis

The structure of CaO NPs was confirmed using XRD techniques. The XRD pattern of CaO is shown in Fig 1. All the observed peaks on XRD profile are in good agreement with the standard JCPDS data (File no. 00-004-0777). This confirmed the cubic phase exhibited by the prepared CaO. Some calcite peaks are observed in the pattern. This may be due to rapid carbonation reaction of CaO by atmospheric CO_2 . This process occurs too fast for CaO and also carbonation rate increases with increasing specific surface area. The average particle size was determined as 48 nm using Scherrer formula.

FTIR Study

The FTIR spectrum of CaO NPs is shown in Fig.2. Three broad peaks were observed from the spectrum. The occurrence of O-H stretching at 3641 cm^{-1} is due to the absorption of moisture present in the atmosphere during the pellet preparation process. The broad band around

1448 cm^{-1} indicates the C-O bond which is associated with carbonation of CaO NPs. The Ca-O metal oxide stretching is observed at 628 cm^{-1} . This is used to confirm the formation CaO NPs.

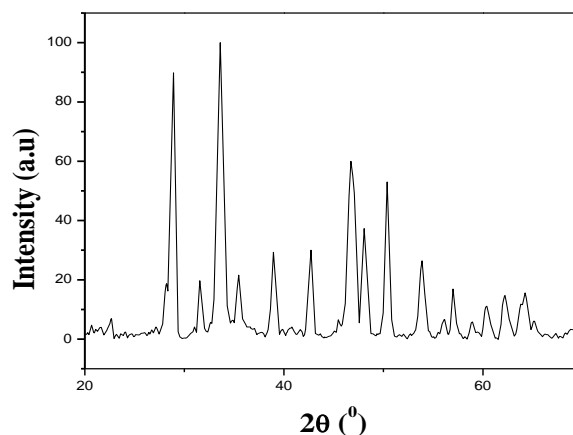


Figure 1: XRD pattern of CaO NPs

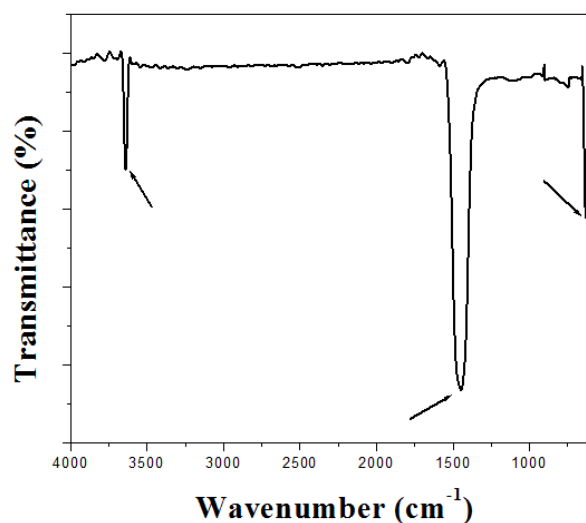


Figure 2: FTIR spectrum of CaO NPs

Transmission Electron Microscope study

The morphology and size of the prepared CaO was analysed using TEM. The TEM micrograph indicates that NPs are irregular in shape as shown in Fig.3. The particle size is varied from 10 nm to 50 nm which is in good agreement with calculated values.

Steady state fluorescence analysis

The intrinsic fluorescence spectra of BSA and BSA- CaO NP complex at excitation wavelength 290 nm are shown in Fig. 4. This excitation wavelength was used for BSA- metal oxide NPs interaction studies earlier.¹¹ Emission maximum of BSA is at 343 nm and fluorescence spectrum of native BSA is different than that of BSA- CaO NP complex. With increasing concentrations of CaO NPs in BSA a gradual decrease in fluorescence intensity with blue shift in emission maximum of BSA was observed. This

fluorescence intensity decrease indicates CaO NPs are responsible for quenching the fluorescence of BSA.



Figure 3: TEM micrograph of CaO NPs

A concentration dependent quenching of BSA intrinsic fluorescence intensity suggested that CaO NPs bind to BSA. The shift of emission maximum of BSA to lower wavelengths indicates movement of tryptophan (trp) residues from a hydrophilic environment to a hydrophobic one. The decreased fluorescence intensity with blue shift in emission maximum of BSA at different concentrations of CaO NPs clearly indicates decreased polarity or increased hydrophobicity of the microenvironment surrounding BSA trp residues. NP–protein interaction alters local chemical environment of fluorophores and quenches fluorescence of proteins.¹² Therefore, fluorescence intensity decrease and shift in emission peak indicate interactions between CaO NPs and BSA. Similar results, quenching of intrinsic fluorescence of BSA with blue shift in emission maximum, was reported during BSA interaction studies with increasing concentrations of ZnO NPs¹³ and Al₂O₃ NPs.¹⁴ Quenching of intrinsic fluorescence of BSA with blue shift in emission maximum was reported for Cu NPs,¹⁵ silver NPs,¹⁶ red shift for ZnO NPs¹¹ and no shift for Copper (I) oxide NPs¹⁷ and gold NPs.¹⁸

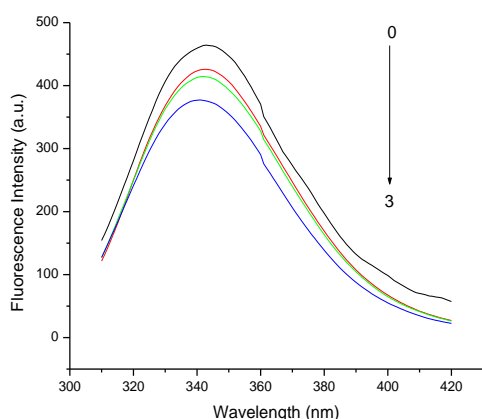


Figure 4: Fluorescence spectra of BSA at different concentrations of CaO NPs (0, 6, 12 and 18 x 10⁻⁸ M)

Time resolved fluorescence analysis

The exponential decay curves of BSA and BSA- CaO NP complex are shown in Fig. 5. The fluorescence decay of BSA were fitted with two exponentials, $T_1 = 6.50$ ns and $T_2 = 2.46$ ns and is consistent with the studies that lifetimes of trp fluorescence are often multi exponential.¹⁹ The marked difference between longer and shorter lifetimes indicated that BSA contained two trp residues that fluoresced in two different environments²⁰ and one of the trp residues in the protein may be buried inside the hydrophobic interior of the protein whereas the other trp residue may be close to quencher.²¹ This is in good agreement with the reports that BSA has two tryptophan residues.⁹ The changes in lifetime give information about the local environment of trp-residues.²²

For all three concentrations of CaO NPs fluorescence lifetimes of both trp residues of BSA- CaO NP complex were found to be lower than that of native BSA fluorescence lifetimes. Similar results were observed with decrease in fluorescence lifetime when BSA interacted with TiO₂ NPs and silver NPs.^{23,24} When concentrations of CaO NPs in BSA increased there was a gradual decrease in lifetime T_1 of BSA- CaO NP complex but for lifetime T_2 an increase and then decrease in fluorescence lifetime was observed (Fig. 5 and Table 1). For dynamic quenching lifetime of fluorophore will decrease due to collision between excited protein fluorophore and NPs.¹² Therefore in this case the decrease in fluorescence lifetimes of both trp residues of BSA indicated consistent dynamic quenching process in the BSA- CaO NP complex. This result is consistent with time resolved fluorescence measurements in which dynamic quenching occurred by the interaction of BSA with TiO₂ NPs²³ and silver nanoparticles²⁴. Static quenching mechanism was confirmed by time resolved measurements when BSA interacted with colloidal ZnO NPs,²⁵ SnO₂ NPs²⁶ and no significant change in average lifetime of trp residues with gold NPs.²⁷

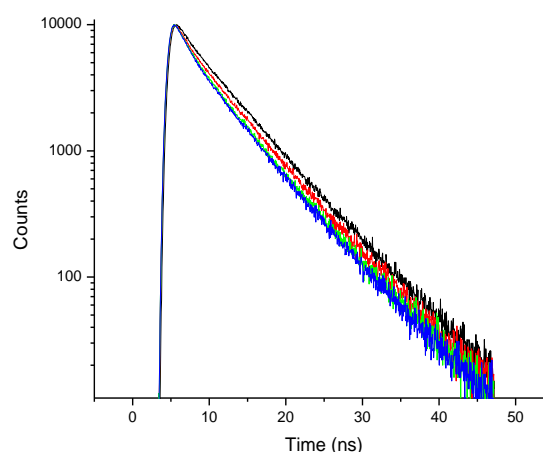


Figure 5: Time resolved fluorescence decay of BSA at different concentrations of CaO NPs (0, 6, 12 and 18 x 10⁻⁸ M)

Conformational changes of BSA - CaO NP complex

The protein NP interaction results in considerable changes of the structure and function of proteins.²⁸ In proteins fluorescence spectrum is determined by the chemical environment of trp hence conformational changes occurs when there are changes in the emission spectra of trp. During BSA- CaO NPs interactions there was a gradual decrease in fluorescence intensity of BSA with a blue shift in fluorescence emission maximum implies conformational changes induced by CaO NPs on BSA. Protein conformational changes will generate some alterations in fluorescence intensity/emission maximum

and disturb microenvironment around trp residues.^{29,30} The fluorescence lifetime of both trp residues in BSA decreased when interacted with all three concentrations of CaO NPs indicating dynamic quenching process. Fluorescence lifetimes are sensitively dependent on protein conformations.²² from the present study, decrease in fluorescence intensity; blue shift in emission maximum and decrease in lifetimes (Fig. 4, Fig. 5 and Table 1) confirmed CaO NPs induced conformational changes in the structure of BSA. Conformational changes were observed when BSA interacted with CuO NPs,³¹ Copper I oxide NPs,¹⁷ Cu NPs¹⁵, ZnO NPs,¹³ colloidal ZnO NPs,²⁵ CdO NPs,³² TiO₂ NPs³³ and tin oxide NPs²³.

Table 1: Emission wavelengths, corresponding fluorescence intensities, lifetimes of BSA and BSA with different concentrations of CaO NPs.

Sample	Emission Maximum(nm)	Fluorescence Intensity (a.u.)	Lifetime T ₁ (ns)	Lifetime T ₂ (ns)
BSA	343	464	6.50	2.46
BSA+6x10 ⁻⁸ M CaO NPs	343	425	6.29	2.11
BSA+12x10 ⁻⁸ M CaO NPs	342	414	6.19	2.16
BSA+18x10 ⁻⁸ M CaO NPs	341	377	6.06	1.85

CONCLUSION

CaO NPs were synthesized by precipitation technique. XRD analysis showed the average particle size as 48 nm. The TEM micrograph showed particles of different size varying from 10 to 50 nm. Fluorescence quenching was confirmed due to decrease in fluorescence intensity of CaO NPs – BSA complex compared to native BSA. A blue shift in emission maximum of BSA was observed while increasing CaO NPs concentrations in BSA. The decreased fluorescence intensity and blue shift in fluorescence emission peak indicated microenvironment close to trp residues of BSA is perturbed. The decreased lifetimes T₁ and T₂ of both trp residues in BSA when interacted with different concentrations of CaO NPs indicated dynamic quenching process. The two lifetimes indicated that BSA contained two trp residues, longer lifetime indicated that trp residue is buried inside hydrophobic interior of protein and shorter lifetime indicted trp residue is closer to quencher. Thus it is concluded that CaO NPs induced conformational changes in the structure of BSA.

REFERENCES

1. Ranghar S, Nanoparticle-based drug delivery systems: promising approaches against infections, *Braz Arch Biol Techn.*, 57, 2013, 209–222.
<http://dx.doi.org/10.1590/S1516-89132013005000011>
2. Seigneure R, Markey L, Nuyten DSA, Dubernet C, Evelo CTA, Finot E, Garrido C, From nanotechnology to nanomedicine: applications to cancer research, *Curr Mol Med.*, 10, 2010, 640–652. doi: 10.2174/156652410792630634
3. Abed N, Couvreur P, Nanocarriers for antibiotics: a promising solution to treat intracellular bacterial infections, *Int J Antimicrob Agents*, 43, 2014, 485–496.
doi:10.1016/j.ijantimicag.2014.02.009
4. Bae DH, Yeon JH, Park SY, Bactericidal Effect of CaO (Scallop-Shell powder) on Foodborne Pathogenic Bacteria, *Archives of Pharmacal Research*, 29, 2006, 298–301.
doi:10.1007/BF02968574
5. Wang L, Hu C, Shao L, The antimicrobial activity of nanoparticles: present situation and prospects for future, *International Journal of Nanomedicine*, 12, 2017, 1227–1249.
<http://dx.doi.org/10.2147/IJN.S121956>
6. Sawai J, Quantitative evaluation of antibacterial activities of metallic oxide powders (ZnO, MgO and CaO) by conductimetric assay, *Journal of Microbiological Methods*, 54, 2003, 177–82. doi:10.1016/S0167-7012(03)00037-X
7. Butt AR, Ejaz S, Baron JC, Ikram M, Ali S, CaO nanoparticles as a potential drug delivery agent for biomedical applications, *Digest Journal of Nanomaterials and Biostructures*, 10, 2015, 799 – 809
8. Gedda G, Pandey S, Yu-Chih Lina, Hui-Fen Wu, Antibacterial effect of calcium oxide nano-plates fabricated from shrimp shells, *The Royal Society of Chemistry Green Chem*, 2015, DOI: 10.1039/c5gc00615e
9. Jung Se H, Choi SJ, Kim HJ, Molecular characteristics of bovine serum albumin-dextran conjugates. *Biosci Biotechnol Biochem*, 70, 2006, 2064–2070.
<https://doi.org/10.1271/bbb.60026>



10. Monopoli MP, Aberg C, Salvati A, Dawson KA, Biomolecular coronas provide the biological identity of nanosized materials, *Nat Nano*, 7, 2012, 779–786. doi:10.1038/nnano.2012.207
11. Bhunia AK, Samanta PK, Saha S, Kamilya T, ZnO nanoparticle-protein interaction: Corona formation with associated unfolding, *Applied Physics Letters*, 103, 2013, 143701. <https://doi.org/10.1063/1.482401>
12. Lakowicz JR, Principles of fluorescence spectroscopy. 3rd edn Springer New York, 2006, 277–330
13. Bhogale A, Patel N, Sarpotdar P, Mariam J, Dongre PM, Miotello A, Kothari DC, Systematic investigation on the interaction of bovine serum albumin with ZnO nanoparticles using fluorescence spectroscopy, *Colloids Surf B*, 102, 2013, 257–264.
doi: 10.1016/j.colsurfb.2012.08.023
14. Abraham S, Effect of Al₂O₃ nanoparticles on bovine serum albumin: A spectrofluorometric study. *Asian Journal of Chemistry*, 29, 2017, 821-824. <https://doi.org/10.14233/ajchem.2017.20321>
15. Latheef SAA, Chakravarthy G, Mallaiah D, Spectroscopic and computational analysis of protein binding on copper nanoparticles: an insight into ligand and nanocarrier interaction, *Journal of Applied Spectroscopy*, 83, 2016, 896-902.
doi: 10.1007/s10812-016-0381-3
16. Mariam J, Dongre PM, Kothari DC, Study of interaction of silver nanoparticles with bovine serum albumin using fluorescence spectroscopy, *J Fluoresc*, 21, 2011, 2193–2199. doi: 10.1007/s10895-011-0922-3
17. Maity M, Pramanik SK, Pal U, Copper (I) oxide nanoparticle and tryptophan as its biological conjugate: a modulation of cytotoxic effects, *J Nanopart Res*, 16, 2014, 2179.
doi: 10.1007/s11051-013-2179-z
18. Shang L, Wang YZ, Jiang JG, pH-dependent protein conformational changes in albumin: Gold nanoparticle bioconjugates: A spectroscopic study, *Langmuir*, 23, 2007, 2714–2721. doi: 10.1021/la062064e
19. Kelkar DA, Chaudhuri A, Haldar S, Chattopadhyay A, Exploring tryptophan dynamics in acid-induced molten globule state of bovine alpha lactalbumin: a wavelength-selective fluorescence approach, *Eur Biophys J*, 39, 2010, 1453-1463.
doi: 10.1007/s00249-010-0603-1
20. De-Llanos R, Sa´nchez-Cortez S, Domingo C, Surface plasmon effects on the binding of antitumoral drug emodin to bovine serum albumin, *J Phys Chem C*, 115, 2011, 12419– 12429. doi: 10.1021/jp111683c
21. Johansson JS, Binding of the volatile anesthetic chloroform to albumin demonstrated using tryptophan fluorescence quenching, *J Biol Chem*, 272, 1997, 17961–17965. <https://doi.org/10.1074/jbc.272.29.17961>
22. Lakowicz JR, Principles of fluorescence spectroscopy. 2nd edn Kluwer Academic Publishers Dordrecht, 1999.
23. Togashi DM, Ryder AG, Mahon DM, Dunne P, McManus J, Fluorescence study of bovine serum albumin and Ti and Sn oxide nanoparticles Interactions. *Proc of SPIE-OSA Biomedical Optics*, 6628, 2007, 1605-1622. <https://doi.org/10.1364/ECBO.2007.6628-61>
24. Voicescu M, Ionescu S, Daniel GA, Spectroscopic and coarse-grained simulation studies of BSA and HSA protein adsorption on silver nanoparticles, *J Nanopart Res*, 14, 2012, 1174. <https://doi.org/10.1007/s11051-012-1174-0>
25. Kathiravan A, Paramaguru G, Renganathan R, Study on the binding of colloidal zinc oxide nanoparticles with bovine serum albumin, *J Mol Struct*, 934, 2009, 129-134.
a. doi: 10.1016/j.molstruc.2009.06.032
26. Gao XY, Wen W, Song ZY, Zhang AP, Hao J, Huang Q, Effects of rare earth ions on the interaction between nano TiO₂ and bovine serum albumin in the presence of ultrasound, *Acta Phys Chim Sin*, 28, 2012, 417- 422. doi: 10.3866/PKU.WHXB201112051
27. Ojha K, Chowdhury PK, Ganguly AK, Fluorescence and CD studies of protein denaturation in the presence of sub picomolar gold nanoparticles, *Indian Journal of Chemistry*, 51, 2012, 1561- 1566. <http://hdl.handle.net/123456789/14892>
28. Walkey CD, Chan WC, Understanding and controlling the interaction of nanomaterials with proteins in a physiological environment, *Chem Soc Rev*, 41, 2012, 2780-2799. doi:10.1039/C1CS15233E
29. Garg A, Manidhar DM, Gokara M, Malleda C, Reddy CS, Elucidation of the binding mechanism of coumarin derivatives with human serum albumin, *Plos One* 8, 2013, e63805. <https://doi.org/10.1371/journal.pone.0063805>
30. Soares S, Mateus N, De Freitas V, Interaction of different polyphenols with bovine serum albumin and human salivary α-amylase by fluorescence quenching, *J Agr Food Chem*, 55, 2007, 6726–6735. <https://doi.org/10.1021/jf070905x>
31. Esfandfar P, Falahati M, Saboury AA, Spectroscopic studies of interaction between CuO nanoparticles and bovine serum albumin, *Journal of biomolecular structure and dynamics*, 2015, 1096213. <https://doi.org/10.1080/07391102.2015.1096213>
32. Abraham S, Sarathy VP, Effect of CdO nanoparticles on bovine serum albumin: A spectrofluorometric study, *Asian Journal of Chemistry*, 28, 2016, 2435-2440. <http://dx.doi.org/10.14233/ajchem.2016.20007>
33. Kathiravan A, Renganathan R, Interaction of colloidal TiO₂ with bovine serum albumin: A fluorescence quenching study, *Colloids and Surfaces A: Physicochem. Eng. Aspects*, 324, 2008, 176–180.
<https://doi.org/10.1016/j.colsurfa.2008.04.017>

Source of Support: Nil, Conflict of Interest: None.

